Journal of Wasit for Science and Medicine 2026: 19, (2), 13-26

Development of An Ionosphere Monitoring Sensors Placed on Nanosatellites

Shaimaa Hussein Shahad [a], Ali Noori Mohammed [b], and Firas Mohammad Dashoor [a]

Department of Physics, College of Science, Wasit University, Wasit, Iraq. [a]
Ministry of Oil, Baghdad Oil Training Institute (BOTI), Baghdad, Iraq. [b]

Abstract

The significance and difficulties of instrumental research on density of the upper atmosphere (ionosphere) such as the composition are discussed. Coupling the density and the ionic composition sensor for high atmosphere, mounted on nanosatellites, are suggested as a solution to these issues. A rough idea for a compact combined converter of the higher atmospheric layers' density and ionic composition is provided. The primary characteristics of the sensor were established based on modeling the ionization processes in the working region of the vacuum transducer and the electron-ion trap.

Keywords: Ionosphere, Density, Ionic Composition, Sensor, and Modeling.

1. Introduction

Understanding the intricate processes taking place in the ionosphere because of solar and galactic radiation requires measurements of the ionosphere's composition and density. The forecast how the Earth's ecosystem will evolve in the future, to study how it will interact with solar radiation and the nearby space, to study the effects of anthropogenic activity on it, and to further explore the nearby space, which is becoming increasingly important to human economic activity. However, the atmosphere density and its compositions were only directly measured within heights between 30-70 km, or at the troposphere–stratosphere range, using equipment mounted on high-altitude aircraft, geophysical research, rockets, and stratospheric balloons [1].

The atoms ionization leads in a much higher concentration of electrons and ions

in the ionosphere. High content electrons and ions in the ionosphere are distorted by the presence of a geomagnetic field, resulting in cyclotron rotations along the force lines of the field [2]. The ionosphere dramatically changes morphing as the day, season, and solar cycle progress. It is subject to ionospheric electric currents and wave processes [3, 4]. Following these shifts and how they vary with location, season, time of day, and solar activity is essential for developing models of the upper atmosphere's condition and understanding its processes in greater depth.

This is why manned and unmanned satellite-borne scientific instruments are essential for conducting direct local analyses of the air density and its compositions at these altitudes [5]. Between 80 and 400 km, where manned spacecraft orbit, the atmosphere undergoes its most dramatic processes in response to solar and galactic radiation. These altitudes exceed 350-400 kilometres. Hence, research equipment fitted on micro- and nanosatellites that are launched from the International Space Station (ISS) or from spacecraft (manned or unmanned) that orbit the earth in progressively decreasing orbits for months can play an important role at these altitudes. Unfortunately, they are susceptible to mechanical failure and vibration because of their lack of durability. It is essential to conduct local and direct analyses by specific instrumentsof the air density and its compositions at these altitudes utilizing both manned and unmanned satellite-borne scientific equipment [5, 6]. At the (80 - 400) km altitude range, where manned spacecraft orbit, the atmosphere's most significant processes involving the interaction with solar and galactic radiation occur. This is space that is greater than (350 - 400) kilometres in altitude.

Equipment deployed on micro- and Nanosatellites that are launched from the International Space Station (ISS) or spacecraft (manned or unmanned) and spin about the Earth in progressively decreasing orbits for months can therefore play a key role in research at these altitudes. Current industrial ionization vacuum gauges are not suitable for these applications because of their low mechanical strength, limited vibration resistance, and excessive power requirements from the power source. However, the effect that charged particles have on the data collected by these sensors.

2. Methodology

2.1 Designing a Combined Transducer for Measuring the Density and Composition of the Upper Atmosphere

A cold cathode inverse magnetron is the optimal configuration for an ionization vacuum transducer operating in the ionosphere. Higher vibration resistance, mechanical strength, and decreased power consumption when detecting pressure from ($1\text{-}10^{-6}$) Pa, which refers to altitudes range of (80 - 500) km [1].

The principal downsides of using industrial sensors in micro- and Nanosatellites are their bulky design, heavyweight, and excessive power requirements due to energy losses. Nonetheless, workarounds exist for these issues. Due to the extremely high concentration of charged particles at these altitudes, it is exceedingly impossible to completely rule out their influence on its results. The entry of charged particles from the external environment into the core might cause the readings to be significantly distorted, especially given the negligible neutral particle ionization coefficient in the converter's active zone (on the order of 10^{-6}).

A charged particle trap must be integrated into this converter to prevent harmful ions and electrons from entering the vacuum converter's working region. The content of positively and negatively charged particles can be independently determined in case the currents measured by the neutral particles by the trap electrodes as shown in figure 1.

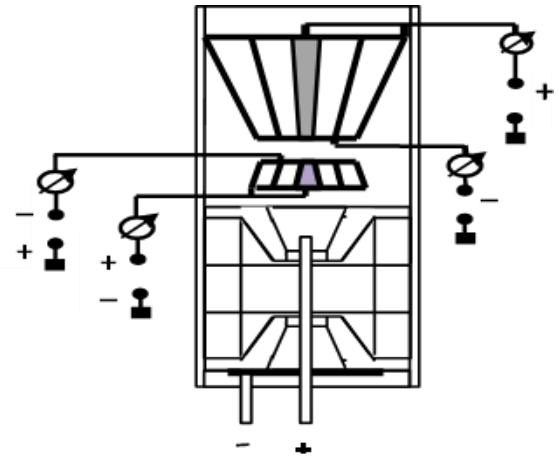

Figure 1: The design of the combined sensor for ionosphere research.

Vacuum transducer magnets are made up of three Armco iron pole plates and three neodymium magnets that are round and longitudinally magnetized but joined by their opposite poles. In this configuration, the cathode of the inverse magnetron vacuum transducer is formed without the need for any extra fastening other than the attraction between the rings and between the rings and the pole pads.

The electron-ion trap design as part of the combined converter consists of two systems of electrodes, which are thin-

walled cones nested into each other. In this case, the gaps of the upper system of electrodes narrow with height change that leads to an increase in the strength of the electric field as the charged particle penetrate deep into the trap. The trap electrode systems are powered from the same source as the vacuum transducer. The height of the upper system of electrodes and the gaps between them are chosen from the condition of neutralization of all charged particles with energy up to approximately 40 keV. The transverse dimensions of the trap are determined by the transverse dimensions of the vacuum transducer (even those whose initial velocity is directed along the gaps between electrodes). Trial computations were used to calculate the trap electrodes' geometrical dimensions. The upper electrode system is 30 mm tall. Except the core electrodes, the electrodes themselves can be manufactured by stamping brass with a thickness of (0.1-0.2) mm. The electrodes in the centre are solid. 10 mm exists between the upper and lower electrode systems, all of trap electrodes geometrical dimensions were listed in table 1.

Table 1: Geometric dimension strap electrodes.

Item	No. Cone	1	2	3
Upper Electrode system	Upper, mm	19	13	7
	Lower, mm	10	6	2
Lower Electrode system	Upper, mm	10	6	2
	Lower, mm	13	9	5

2.2 Determination of the electric field and currents of a vacuum transducer

In ionization vacuum converters, neutral particles become ionized through inelastic electron collisions. "Seed" electrons are formed in the active zone of the converter when an electron-ion trap is present, preventing free electrons from the environment from entering.

These electrons are released from the magnet's wall layers and the pole pads when gamma and X-rays interact with them (at heights higher than earth surface). In the presence of magnetic and electric forces, unbound electrons will move in cyclical patterns. The average electron velocity is calculated by adding the thermal (chaotic) and drift velocities, and the electron energy is calculated in the same way. Since electrons get more energy from the electric

field, the electron drift velocity is critical for ionization.

Its speed is determined not only by the magnitude of the electric field but also by the ratio of the cyclotron frequency (the rate at which electrons rotate in a magnetic field) to the frequency at which they collide with particles of a neutral gas (v_{en}). This ratio establishes the interval between collisions for the electron, measured in terms of its rotating cycles. Furthermore, to establish the drift velocity of electrons, the cyclotron rotation frequency (ω_c) and the frequency should both known at which they collide with neutral particles (v_{en}).

$$\left[\omega_c = \frac{eB}{m_e} = \frac{1.6 \times 10^{-19}}{0.911 \times 10^{-30}} B = 1.756 \times 10^{11}.B\right] \quad (1)$$

Substituting the value of the magnetic induction = 0.1 T,ω_c= 1,756×10^{11}×0,1 = 1,756×10^{10} [s^{-1}].

The mean neutral gas particle-free route is approximately equal to the mean electron-free path (denoted by le) under identical conditions. When comparing heights of 150 to 500 km, the neutral gas particle's free path is between 3.37 m and 14.7 km. If this is the case, the electrons mean free path will be anywhere between 19 meters and 83 kilometres. Although the dimensions of the interelectrode space are bigger than those of the active zone. Entirely acceptable to view this motion of free electrons in a vacuum in the presence of adequate electric and magnetic fields as occurring within the converter. Electronic drift velocity and energy can now be calculated from equation two.

$$\left[V_d = \frac{e}{m_e} \cdot \frac{E}{v_{en}\sqrt{1 + \frac{\omega_c^2}{v_{en}^2}}}\right] (2)$$

Cyclotron rotation frequency denoted as e. The air gap induction and its strength are the only two factors that determine the number of electrons. The speed of light, e, is equal to 1.756 1010 s-1 when B = 0.1 T. Hence, equation two is replaced with equation three.

$$\left[V_d = 1.756 \times 10^{11} \frac{E}{1{,}756 \cdot 10^{10}} = 10E\right] (3)$$

The drift energy of electrons may be easily calculated using the values of drift velocity Vd and the conversion factor Kd = 0.625.1019 from J to eV.

$$\left[\varepsilon_d = \frac{T_e \cdot V_d^2}{2} \times 0.625 \times 10^{19} = 0.285 \times 10^{-11} V_d^2\right] (4)$$

Hence, the average radius of the (Larmor-cyclotron) orbits of the rotation of electrons

in a transverse magnetic field can be calculated as in Eq. 5:

$$[r_c = V_d/\omega_c] \quad (5)$$

The electric field in the converter's operating area can be calculated. The anode and cathode of the converter are coaxially arranged; the electric field strength may be determined using the following formula.

$$\left[E = \frac{U}{rln\,\frac{R_2}{R_1}}\right] \quad (6)$$

The anode radius is $R_1 = 0.75\,mm$ and the cathode radius is$R_2 = 6.3\,mm$. It was found that an anode voltage of 1000 V was adequate for producing an electric field strong enough to cause impact ionization of neutral atoms in the converter's working area. Figure two displays findings of measuring the electric field in the central section's interelectrode space.

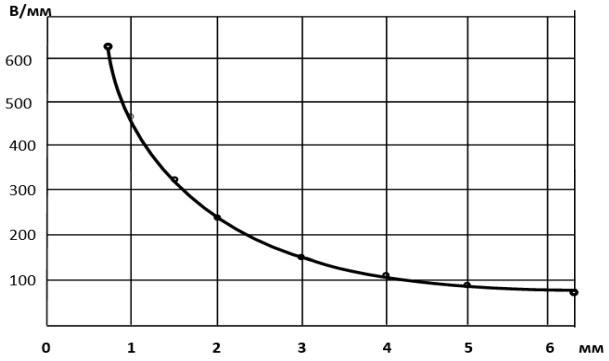

Figure 2: Electric field strength dependence on the current radius.

Computed values for the cyclotron orbit radius, drift energy d and drift velocity v_d are listed in (table 2). The air threshold ionization energy is 33.9 eV or the ratio of the ionization energies of nitrogen and oxygen. Considering the dependence of the air ionization cross-section on the electron energy, the maximum ionization probability occurs at a current radius range of 0.8 - 1.5 mm (while the radii of the electrons' cyclotron orbits are between (0.2 and 0.15) mm). Thus, when the converter core current radius is less than 2 mm, direct single-stage ionization of air by electrons will be conceivable.

Table 2: Radius and energy of electron drift, electron drift velocity and electron cyclotron orbits.

r, mm	0.8	1.0	1.5	2.0	3	4	5	6
E.$10^5, B/m$	5	4.7	3.13	2.35	1.57	1.17	0.94	0.75
$V_{de}, 10^5, m/s$	50	47	31.3	23.5	15.7	11.3	9.4	7.5
ε_{de}, eV	71.3	63	56	31.5	14	7.6	5	3.2
r_{ce}, mm	0.28	0.26	0.18	0.14	0.09	0.06	0.05	0.04

Although multi-stage ionization would also occur, just the first stage is considered here. The ionization potential of excited molecules drops according to the energy with which they became excited. At electron energies, the multisteps ionization mechanism occurs, there is a substantial possibility that air molecules will be excited

(2 eV). In this case, the number of excited electrons collide with neutral particles is larger than the number of ionization collisions for both electrons with energies above and below the ionization potential.

Even though the lifetime of excited molecules is often short (on the order of 108s) [1, 7], it is possible to excite metastable states with lifetimes much longer than 1 s for both oxygen and nitrogen molecules, and the cross-section of these reactions is large (about = 10 barns). Ionization can occur in multiple stages throughout the vast majority of the converter's active zone [8].

In active zone, neutral atoms of an inverse-magnetron converter are gradually ionized as time passes like an avalanche because after an ionization collision between an electron and a neutral particle [8], an additional electron is knocked out of each particle. There is an avalanche-like increase in the number of ionization collisions until a dynamic equilibrium between the number of positive ion pairs generated per unit of time and the number of ions and electrons neutralized at the converter cathode and anode is reached.

As the external circuit for both the electronic and ionic currents is closed, it follows that two currents are identical. It is then possible to estimate the average lifetime I_{av} of an ion, given its drift velocity v_{di} and the period between its birth and neutralization at the cathode, I_{av} [1].

The drift velocity of the ion is proportional to core current radius of the converter. However, because the maximum ionization zone coincides with values of the current radius between (1 mm and 2 mm), the value equivalent to the current radius of 1.5 mm and equal to v_{di} = 31.3 105 m / s as listed in (table 1), and the distance between this zone and the inner surface of the cathode, I_{av} (6 -1.5) = 4.5 mm, as an average path length. Putting these numbers into equation seven leads to [1].

$$\left[\tau_i = \frac{4{,}5 \times 10^{-3}}{313 \times 10^{5}} = 1.438 \times 10^{-9} \approx 1.44 \times 10^{-9} s\right] \quad (7)$$

As the ion current depends on the pressure Ii = (p), ions number can be estimated entering the converter cathode per unit of time.

$$\left[\tau_i = \frac{l_{av}}{V_{dav}}\right] (8)$$

$$\left[N_i^i = \frac{I}{e}\right] (9)$$

where I denote that instead of calculating the density of ions (i.e., their quantity per unit volume), ions arrive at the cathode of the converter in a certain amount of time can measured. Finding the

equilibrium of free ions in the active zone plasma of the N_i^v converter [8] is possible if one assumes that newly formed ions travel directly from the anode to the cathode (without undergoing cyclotron rotations).

$$\left[N_i^v = N_i^i \cdot \tau_i\right] (10)$$

This number must be divided by the converter core's volume V to get the average bulk density.

$$\left[N_i = \frac{N_i^v}{V}\right] (11)$$

The active zone of the transducer is a cylinder with an outside diameter of D = 12.7 mm and an inner diameter of d = 2 mm. The distance between the pole plates determines the height of the core, hence H = 10 mm. Hence, its volume will be uniform

$$V = \frac{\pi}{4}(D_n^2 - d_n^2)H = \frac{3.14}{4}(12.7^2 - 2^2) \times 10.6 = 1308MM^3 = 1.308cm^3 \quad (12)$$

$$k_i = \frac{N_i}{N_n} \quad (13)$$

The ionization coefficient for gas molecules in the converter's active zone can be calculated by dividing the steady-state number of ions generated in the active zone by the number of neutral particles in this volume [8, 9].

The vacuum chamber at the Kursk plant «Mayak» was used for experimental tests of the converter to ascertain the true values of the ionization coefficient (10-6 Pa). Pressures range from 5 104 to 0.5 106 Pa at altitudes of 150–500 km. The experimentally determined values of the ionic current and the ionization coefficient are listed in table 3. It's clear that the ionization coefficient is quite tiny, and it drops monotonically with increasing pressure (albeit insignificantly). Since the chance of electron-ion recombination rises with increasing pressure [1, 10].

Table 3: Ionic current and ionization coefficient for pressures (10^{-6}-10^{-3}) *Pa*.

P,p_a	10^{-6}	10^{-5}	10^{-4}	10^{-3}
I, n_A	13.2	128	1.25×10^3	1.23×10^3
N_i^V	49.5	4.8×10^2	4.7×10^3	4.7×10^4
N_n^V	4.6×10^7	7×10^8	9×10^9	1.5×10^{11}
k_i	11×10^{-7}	6.8×10^{-7}	5.2×10^{-7}	3.1×10^{-7}

2.3 Computation of an electron-ion trap's electric fields and currents

The electric field in the coaxial cylindrical system of electrodes is calculated using an approximate analytical method utilizing the formula (6) above because great accuracy of computations is not necessary. Electrodes in this case are

conical rather than cylindrical and the distance between them narrows as height increases. Also, to divide the entire system of electrodes into 10 sections, each with a height of 3 mm, diameters of electrodes were calculated for each of these sections' average (height) sections.

Outcomes of computing the field for the outer pair of electrodes (the dependences for the outer electrode, the inner electrode, and the middle of the gap between them are shown in figure three. The moment T when the particle reaches the opposite electrode is calculated from the condition, where d is the width of the gap between the electrodes, so particles falling perpendicular to the direction of the field and close to a similarly charged electrode will have the largest range.

$$T = \sqrt{\frac{2md}{qE}} \quad (14)$$

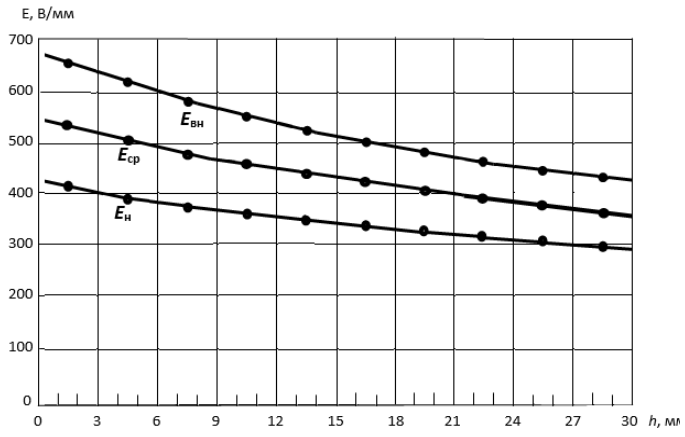

Figure 3: Dependencies $E = f(h)$ for the outer pair of electrodes.

Supposing that during the time *T,* the velocity of the particle along the z-axis remains unchanged and is equal to *V*, the current height of the trap $h = VT$ at which the particle will reach the opposite electrode [3, 8].

$$h = V\sqrt{\frac{2md}{qE}} \quad (15)$$

Transition from velocity to particle energy $E_{kin} = (mV^2)/2$, whence $V = \sqrt{\frac{2E_{kin}}{m}}$ and substituting this expression instead of the velocity in the formula for *h*, can obtain

$$h_T = \sqrt{\frac{4E_{kin}d}{qE}} \quad (16)$$

Finding particles from this E_{kin}, can obtain

$$E_{kin} = \frac{h_T^2 qE}{4d} \quad (17)$$

If there instead of the current height h_T, the substitute the total height of the trap *H*, then results the limiting kinetic energy of particles captured by this trap, in the most unfavourable case, when their velocity is directed along the gap between the trap electrodes:

$$E_{kinmax} = \frac{H^2 qE}{4d} \quad (18)$$

The gap width d and the field strength *E* along the path of the particle will change. But, since the work interested in the approximate values of the energy, the

calculation will be carried out for their average values both for the height of the trap and for the width of the gap for each pair of upper electrodes. Considering these assumptions and considering the conversion factor from joules to electron volts: Kp = $6.25 \cdot 10^{18}$ the outer pair of electrodes.

$$E_{kinmax} = \frac{30^2 \times 1.6 \times 10^{-19} \times 450}{4 \times 2.5} = 6.48 \times 10^{-15}\, j = 40.5\, K\, eV \quad (19)$$

For the inner pair of electrodes.

$$E_{kinmax} = \frac{30^2 \times 1{,}6 \times 10^{-19} \times 500}{4 \times 2{,}5} = 7.2 \times 10^{-15}\, j = 45\, K\, eV \quad (20)$$

The modest rise in the average value of the electric field between the inner pair of electrodes is all that accounts for the little difference (due to a decrease in the average diameters of the electrodes). It is important to know the altitude distribution of the density of all types of charged particles and their energy at altitudes of (150-500) km to calculate the currents of an electron-ion trap. Will compute the energy for the rms velocities in this scenario because the particle velocities with the constancy of the other parameters are distributed by the Maxwell-Boltzmann law in a reasonably large range. In table (4) some basic parameters of the atmosphere at altitudes (150-500km) are shown. At thermodynamic equilibrium, the average energy of particles at all heights does not surpass a few electron volts. The upper electrode system will therefore ensure that they are all neutralized. The calculation of the upper system currents of the trap electrodes will be done for conditions of thermodynamic equilibrium with the medium, where the thermal motion of air molecules moves at a rate that is several times slower than the satellite's orbital speed, which in low orbits is roughly equal to 8000 m/s. The equilibrium electron velocities, however, will be four orders of magnitude more than the satellite's speed. It is possible to ignore their own thermal speed when calculating the speed of air molecules and ions relative to the trap, and their own satellite speed can be disregarded when calculating the speed of electrons relative to the trap. Consequently, the relative velocity equal to Vl = 8000 m/s for computing the number of ions entering the trap.

Table 4: Basic parameters of the atmosphere at altitudes of (150- 500) km.

Z, KM	150	200	250	300	400	500
T, K	800	900	1000	1100	1400	1950
P, pa	7.7×10^{4}	9.9×10^{-5}	5.5×10^{-5}	1.1×10^{-5}	0.95×10^{-6}	0.55×10^{-6}
N_n, CM^{-3}	7×10^{10}	8×10^{9}	2×10^{9}	7×10^{8}	5×10^{7}	2×10^{7}
N_e, CM^{-3}	1×10^{5}	1×10^{5}	1×10^{6}	1×10^{6}	1×10^{6}	4×10^{5}
V_{kB}, m/s	812	861	908	952	1073	1268
E_{kB}, ev	0.98	1.1	1.23	1.35	1.71	5.67
λ_{avg}, m	3.37	29.5	143	337	4.7×10^{3}	14.7×10^{3}
V_{nn}, c^{-1}	222	26.9	5.85	2.33	0.21	0.079
V_{en}, c^{-1}	910	150	47	18	3.5	0.9
V_{ei}, c^{-1}	480	440	650	810	590	300
V_{in}, c^{-1}	60	6	2	0.7	0.2	0.05

The trap is immobile while estimating the number of electrons falling into it. Also presume that the plasma is electrically neutral at all altitudes, meaning that the concentrations of ions and electrons are constant everywhere. Taking this into account, the number of ions trapped in 1 s at different heights will be determined as, where N_i^h, is the concentration of ions at the height h, Sl is the area of the upper section of the gaps between the pairs of electrodes of the upper electrode system, V_l is the orbital velocity of the trap.

Since the research is only interested in the range of variation of the trap currents, from the data in table 3. Only the maximum and minimum values of the ion concentration are used. The spread here is not large (only tenfold, in contrast to the range of variations in the concentration of neutral particles, which is three orders of magnitude). Accordingly, to obtained.

$$N_{imin}^h = 1 \times 10^{-6} \times 2.4 \times 8 \times 10^5 \approx 1.9 \quad (21)$$

$$N_{imax}^h = 1 \times 10^{-5} \times 2.4 \times 8 \times 10^5 \approx 19 \quad (22)$$

Assuming all ions to be singly charged, the minimum value of the ion current will be

$I_{imin} = N_{imin} \cdot q_e = 1.9 \times 10^{11} \times 1.6 \times 10^{-19}$ = 30 nA, and the maximum is 300 nA.

The determination the electron current involve the number of electrons falling into the trap in 1 second will be significantly higher than the number of ions, even though the concentrations of positive ions and electrons at each altitude will be assumed to be the same. This is because of the stark difference in the velocities of the particles relative to the trap. However, because electrons have tens of thousands of times less mass than ions, the speed at which they drift in the trap's electric field should likewise increase by this similar amount [11, 12]. Calculations indicated that it should move at a speed several orders of magnitude faster than light. As it can only approximate the speed of light. The length of their existence, on average, from the time they enter the trap until they are neutralized at the positive electrodes will be.

$$\tau_{avg} = \frac{l_{avg}}{V_{de}} = \frac{2.5 \times 10^{-3}}{3 \times 10^{8}} = 0.83 \times 10^{-11} s \quad (23)$$

$$\tau_{eavg} = \frac{l_{avg}}{V_{de}} = \frac{2.5 \times 10^{-3}}{3 \times 10^{8}} = 0.83 \times 10^{-11} c \quad (24)$$

The loss of electrons will be continuously replenished from the external environment, i.e., the minimum and maximum number of electrons neutralized in the trap in 1 second will be.

$$N_{e/s} = \frac{N_{e\,min}}{\tau_{e\,avg}} = \frac{1.9}{0.831 \times 0^{-11}} = 2.3 \times 10^{11}\, \boldsymbol{s^{-1}} \quad (25)$$

$$N_{e\,max/s} = \frac{N_{e\,min}}{\tau_{e\,\mathrm{cp}}} = 2.3 \times 10^{12} \boldsymbol{s^{-1}} \quad (26)$$

The corresponding currents will be equal to.

$$I_{e\,min} = q_e * N_{\frac{e}{s}} = 1.6 \times 10^{-19} \times 2.3 \times 10^{11} = 3.7 \times 10^{-8}\, A = 37\, n\mathrm{A} \quad (27)$$

$$I_{e\,max} = q_e \times N_{e/s} = 370\, n\mathrm{A} \quad (28)$$

It is extremely difficult to estimate the fraction of high-energy particles not retained by the upper electrode system, but there will be much fewer of them than the particles trapped by the upper electron system because the upper system retains and neutralizes not only all charged particles with energies below 40 keV, but also increasingly energetic particles whose initial velocities are not directed along the gaps between the trap electrodes. As a result, the bottom system of electrodes measuring channels must be as sensitive as possible (at least up to units of Nano amperes).

3. Conclusion

All characteristics of the atmosphere within the ionosphere are highly variable and depend on a variety of variables, including the area's latitude, the time of day, the season, solar activity, and many other variables. Because of this, it is important to develop measuring instruments for taking direct measurements of the composition and density of the upper layers of the atmosphere that can be mounted on micro- and Nano satellites.

The intense rarefaction and high level of ionization in the upper atmosphere are the key constraints limiting the utilization of the industrial devices now in use for these purposes. This is why at these altitudes, specialized scientific tools for analysing the ionosphere's density and composition that are suited for autonomous operation in micro- and Nano satellites can be most useful. A mathematical model for the combined sensor of density and composition of the upper layers of the atmosphere has been proposed, and it is based on this model that the computation of the produced.

The range of currents of this transducer at altitudes of (150 - 500) km was established through simulation of the

magnetic and electric fields in the active zone of the vacuum transducer and the ionization processes of neutral particles by electrons in crossed magnetic and electric fields. Finally, electric fields of an electron-ion trap, particle energies that can be trapped, and potential current ranges from neutralizing charged particles at these altitudes have all been calculated.

4. Referencess

1. Al Kadhimi A. N. M., (2020). Combined Vacuum Sensor for Measuring the Density and Composition of the Ionosphere. Materials Science and Engineering Conference Series. 928, 2, 022058.
2. Drejzin V. E., Al Kadhimi A. N. M., (2020). Modeling Electric and Magnetic Fields in Working Area of Inversed Magnetron Vacuum Gauge Converter to Study Density and Composition of Apper Atmospheric Layers. 2020 International Conference on Industrial Engineering, Applications and Manufacturing (ICIEAM) IEEE. 1-5.
3. Andreeva E. S., Franke S. J., Yeh K. C., and Kunitsyn V. E., (2000). Some features of the equatorial anomaly revealed by ionospheric tomography. Geophysical Research Letters. 27, 16, 2465-2468.
4. Panasyuk M. I., and Novikov L. S., (2007). Model of the cosmos. Scientific information publication: in 2 volumes/ Ed., Physical conditions in outer space. M.: KDU.872.
5. Krivolutsky A. A., Klyuchnikova A. V., Zakharov G. R., Vyushkova T. Yu, and Kuminov A. A., (2006). Dynamical response of the middle atmosphere to solar proton Event of July 2000: Three-dimensional model simulations, Advances in Space Research. 37, (1602-1613).
6. Bilitza D., (2001). International reference ionosphere 2000. Radio Science. 36, 2, 261-275.
7. Protasov Y. S., and Chuvashev S. N., (1993). Physical electronics of gas-discharge devices. Plasma Electronics. Higher School, Moscow.
8. Drejzin V. E., and Al Kadhimi A. N. M., (2021). The Ionization Processes Occurring in the Work Area of the Inverse Magnetron Vacuum Gauge Converter to Study the Density and Composition of Upper Atmosphere. Advances in Automation II: Proceedings of the International Russian Automation Conference, RusAutoConf2020, September 6-12, 2020, Sochi, Russia, Springer International Publishing. 152-161.

9. Voronchev T. A. and Sobolev V. D., (1967). Physical foundations of electrovacuum technology. M., Higher school.
10. Yeh K. C., Franke S. J., Andreeva E. S., and Kunitsyn V. E., (2001). An investigation of motions of the equatorial anomaly crest. Geophysical Research Letters. 28, 24, 4517-4520.
11. Ahmadov R. R., and Kunitsyn V. E., (2004). Simulation of generation and propagation of acoustic gravity waves in the atmosphere during a rocket flight. International Journal of Geomagnetism and Aeronomy. 5, 2, 1-12.
12. Tereshchenko E. D., Khudukon B. Z., Gurevich A. V., Zybin K. P., Frolov V. L., Myasnikov E. N., and Carlson H. C., (2004). Radio tomography and scintillation studies of ionospheric electron density modification caused by a powerful HF-wave and magnetic zenith effect at mid-latitudes. Physics Letters A. 325, 5-6, 381-388.